

Axial Interaction of the $[\text{Ru}_2(\text{CO})_4]^{2+}$ Core with the Aryl C–H Bond: Route to Cyclometalated Compounds Involving a Metal–Metal-Bonded Diruthenium Unit

Sanjib K. Patra and Jitendra K. Bera*

Department of Chemistry, Indian Institute of Technology, Kanpur, 208016 India

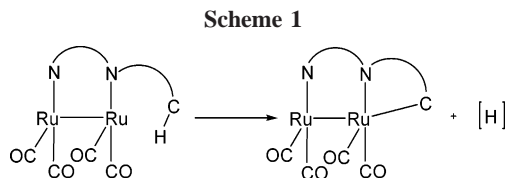
Received August 24, 2006

Room-temperature activation of the aromatic C–H bond by the $[\text{Ru}_2(\text{CO})_4]^{2+}$ core has been achieved. The reactions of 2-phenyl-1,8-naphthyridine (phNP) and 2-(2,5-dimethyl-3-furyl)-1,8-naphthyridine ($\text{Me}_2\text{-fuNP}$) with $[\text{Ru}_2(\text{CO})_4(\text{MeCN})_6][\text{BF}_4]_2$ in dichloromethane provide the agostic-cyclometalated compounds $[\text{Ru}_2(\text{phNP})(\text{C}_6\text{H}_4\text{-NP})(\text{CO})_4][\text{BF}_4]$ (**1**) and $[\text{Ru}_2(\text{Me}_2\text{fuNP})(\text{C}_4\text{OMe}_2\text{-NP})(\text{CO})_4][\text{BF}_4]$ (**2**), respectively. In both compounds, one of the ligands is ortho-metalated, while the second ligand is engaged in an agostic interaction. The ortho metalation is preferred over the potential S coordination for 2-(2-thienyl)-1,8-naphthyridine (thNP), yielding $[\text{Ru}_2(\text{thNP})(\text{C}_4\text{H}_2\text{S-NP})(\text{CO})_4][\text{BF}_4]$ (**3**). In acetonitrile, the compound $[\text{Ru}_2(\text{thNP})_2(\text{CO})_4][\text{BF}_4]_2$ (**4**) is obtained exclusively. The donation of a C–H bonding electron pair to the Ru–Ru σ^* LUMO and back-donation from the filled Ru–Ru π^* orbital to the C–H σ^* orbital cause facile C–H bond cleavage. In contrast, the isoelectronic $[\text{Rh}_2]^{4+}$ provides the agostic compounds $[\text{Rh}_2(\text{OAc})_3(\text{phNP})\text{Cl}]$ (**5**) and $[\text{Rh}_2(\text{L})(\eta^1\text{-L})(\text{OAc})_2(\text{CH}_3\text{CN})_2][\text{BF}_4]_2$ ($\text{L} = \text{phNP, nplNP}$ (2-(2-naphthyl)-1,8-naphthyridine) for compounds **6** and **7**, respectively). The molecular structures of compounds **1–3**, **5**, and **7** have been established by X-ray crystallography.

Introduction

The cyclometalation of aromatic hydrocarbons continues to attract considerable interest, providing valuable insight into C–H bond activation processes.¹ Mononuclear Pd, Pt, Rh, Ir, and Ru complexes are employed frequently for cyclometalation.² This work examines the use of a metal–metal-bonded dimetal unit in the activation of the C–H bond. Cyclometalation reactions of phosphine-based ligands at equatorial sites of the dirhodium unit have been reported at elevated temperature.³ The axial interaction of the $[\text{Ru}–\text{Ru}]^{2+}$ unit with the aryl C–H bond has been investigated in the synthesis of cyclometalated compounds, as shown in Scheme 1.

The diruthenium complex $[\text{Ru}_2(\text{CO})_4(\text{CH}_3\text{CN})_6][\text{BF}_4]_2$ of metal–metal valence configuration⁴ $\sigma^2\pi^4\delta^2\delta^*2\pi^*4\sigma^*0$, corre-



sponding to a formal Ru–Ru single bond, has been employed for this study. The ligands used include 2-phenyl-1,8-naphthyridine (phNP), 2-(2,5-dimethyl-3-furyl)-1,8-naphthyridine ($\text{Me}_2\text{-fuNP}$), and 2-(2-thienyl)-1,8-naphthyridine (thNP) (Chart 1). Room-temperature activation of the C–H bond and subsequent formation of cyclometalated compounds containing the diruthenium unit are presented herein. Similar reactions with the isoelectronic $[\text{Rh}_2]^{4+}$ unit are also reported.

Results and Discussion

Axial Interaction of the $[\text{Ru}_2(\text{CO})_4]^{2+}$ Unit with the Aryl C–H Bond. The aromatic C–H bond is placed at a site trans to the Ru–Ru single bond by utilizing a 1,8-naphthyridine (NP) ligand having the appropriate group covalently attached at the 2-position.⁵ Reactions of phNP, Me_2fuNP , and thNP with $[\text{Ru}_2(\text{CO})_4(\text{CH}_3\text{CN})_6][\text{BF}_4]_2$ in dichloromethane at room temperature resulted in the formation of the red cyclometalated compounds $[\text{Ru}_2(\text{phNP})(\text{C}_6\text{H}_4\text{-NP})(\text{CO})_4][\text{BF}_4]$ (**1**), $[\text{Ru}_2(\text{Me}_2\text{fuNP})(\text{C}_4\text{OMe}_2\text{-NP})(\text{CO})_4][\text{BF}_4]$ (**2**), and $[\text{Ru}_2(\text{thNP})(\text{C}_4\text{H}_2\text{S-NP})(\text{CO})_4][\text{BF}_4]$ (**3**), respectively. The molecular structures of **1–3** have been established by X-ray crystallography. The important metrical parameters are compared in Table 1.

(4) (a) Cotton, F. A.; Murillo, C. A.; Walton, R. A. *Multiple Bonds Between Metal Atoms*, 3rd ed.; Springer: New York, 2005. (b) Cotton, F. A.; Walton, R. A. *Multiple Bonds Between Metal Atoms*, 2nd ed.; Clarendon Press: Oxford, U.K., 1993.

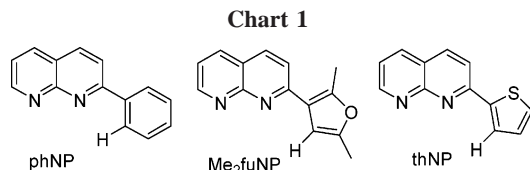
(5) Patra, S. K.; Sadhukhan, N.; Bera, J. K. *Inorg. Chem.* **2006**, *45*, 4007.

* To whom correspondence should be addressed. E-mail: jbera@iitk.ac.in.

(1) (a) Crabtree, R. H. *The Organometallic Chemistry of the Transition Metals*, 3rd ed.; Wiley: New York, 2001. (b) Crabtree, R. H. *Dalton Trans.* **2001**, 2437. (c) Labinger, J. A.; Bercaw, J. E. *Nature* **2002**, *417*, 507. (d) Shilov, A. E.; Shul'pin, G. B. *Chem. Rev.* **1997**, *97*, 2879. (e) Arndtsen, B. A.; Bergman, R. G.; Mobley, T. A.; Peterson, T. H. *Acc. Chem. Res.* **1995**, *28*, 154. (f) Ryabov, A. D. *Chem. Rev.* **1990**, *90*, 403. (g) Dyker, J. *Angew. Chem., Int. Ed.* **1999**, *38*, 1698. (h) Crabtree, R. H. *Chem. Rev.* **1985**, *85*, 245.

(2) (a) Dupont, J.; Consorti, C. S.; Spencer, J. *Chem. Rev.* **2005**, *105*, 2527. (b) Newkome, G. R.; Puckett, W. E.; Gupta, V. K.; Kiefer, G. E. *Chem. Rev.* **1986**, *86*, 451. (c) Dehand, J.; Pfeffer, M. *Coord. Chem. Rev.* **1976**, *18*, 327. (d) Bruce, M. I. *Angew. Chem., Int. Ed. Engl.* **1977**, *16*, 73. (e) Omae, I. *Coord. Chem. Rev.* **1980**, *32*, 235. (f) Omae, I. *Chem. Rev.* **1979**, *79*, 287. (g) Parshall, G. W. *Acc. Chem. Res.* **1970**, *3*, 139.

(3) (a) Lloret, J.; Bieger, K.; Estevan, F.; Lahuerta, P.; Hirva, P.; Pérez-Prieto, J.; Sanaú, M. *Organometallics* **2006**, *25*, 5113. (b) Lloret, J.; Estevan, F.; Lahuerta, P.; Hirva, P.; Pérez-Prieto, J.; Sanaú, M. *Organometallics* **2006**, *25*, 3156. (c) Bieger, K.; Estevan, F.; Lahuerta, P.; Lloret, J.; Pérez-Prieto, J.; Sanaú, M.; Siguero, N.; Stiriba, S. E. *Organometallics* **2003**, *22*, 1799. (d) Lahuerta, P.; Paya, J.; Pellinghelli, M. A.; Tiripicchio, A. *Inorg. Chem.* **1992**, *31*, 1224. (e) Taber, D. F.; Malcom, S. C.; Bieger, K.; Lahuerta, P.; da Rocha, Z. N.; Sanaú, M.; Stiriba, S. E.; Pérez-Prieto, J.; Monge, M. A. *J. Am. Chem. Soc.* **1999**, *121*, 860–861. (f) Chakravarty, A. R.; Cotton, F. A.; Tocher, D. A.; Tocher, J. H. *Organometallics* **1985**, *4*, 8.



The structure of **1** reveals that the “ $Ru_2(CO)_4$ ” unit is spanned by two naphthyridine ligands. One of the phNP ligands is cyclometalated, involving Ru2 bonded to the ortho carbon atom C20 of the phenyl fragment and N2 of the naphthyridine unit (Figure 1). The distal N1 atom is bonded to the other ruthenium. The Ru1–Ru2 and Ru2–C20 distances are 2.692(1) and 2.074(5) Å, respectively, and the Ru1–Ru2–C20 angle is 160.52(14)°. The second phNP ligand bridges the diruthenium unit at equatorial sites, and the ortho hydrogen of the phenyl appendage is located in the vicinity of Ru1. The metrical parameters of Ru1–H40 = 2.398 Å (calculated), Ru1–C40 = 2.786(5) Å, and Ru1–H40–C40 = 104.0(3)° are indicative of an agostic interaction.⁶ The torsion angle (N4–C38–C39–C40) of 50.2(7)° between the phenyl and NP planes is the manifestation of the agostic configuration⁷ of the C–H bond with the diruthenium unit. The corresponding value for the ortho-metalated phNP is 7.8(7)°.

The ¹H NMR of compound **1** displays two distinct sets of aromatic signals for the two ligands. The most unusual signal appears as a doublet at δ 9.29 ppm, representing a significant downfield shift as compared to the signal for the free ligand. The shift is in the opposite direction of what is normally observed for the hydrogen strongly bonded to a metal. Thummel et al.⁸ reported a similar downfield shift of the hydrogen lying at the axial site of the isoelectronic $[Rh_2]^{4+}$ unit and offered several possible rationales. We assign the signal to the agostic hydrogen and attribute the downfield shift to the withdrawal of electron density from the C–H bond to the vacant Ru–Ru σ^* orbital. The ¹³C{¹H} NMR exhibits a characteristic signal for the carbon atom directly bonded to the ruthenium at δ 181.2 ppm. All other aromatic carbons appear in the region of δ 121–161 ppm, whereas the carbons of CO exhibit signals in the region δ 200–207 ppm.

With Me₂fuNP, a similar agostic-cyclometalated compound was isolated, $[Ru_2(Me_2fuNP)(C_4OMe_2-NP)(CO)_4][BF_4]$ (**2**) (Figure 2), the key structural parameters of which are comparable to those of **1** with Ru1–Ru2 = 2.6875(6) Å and Ru2–C20 = 2.066(5) Å. The Ru1–H40 (calculated) and Ru1–C40 distances of 2.358 and 2.741(2) Å and Ru1–H40–C40 angle of 103.6-

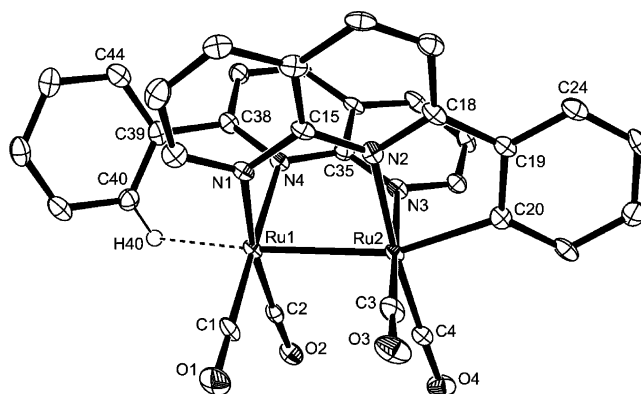


Figure 1. ORTEP diagram (50% probability thermal ellipsoids) of the cationic unit $[Ru_2(phNP)(C_6H_4-NP)(CO)_4]^+$ in compound **1** with important atoms labeled. Hydrogen atoms, except for the agostic hydrogen, are omitted for the sake of clarity.

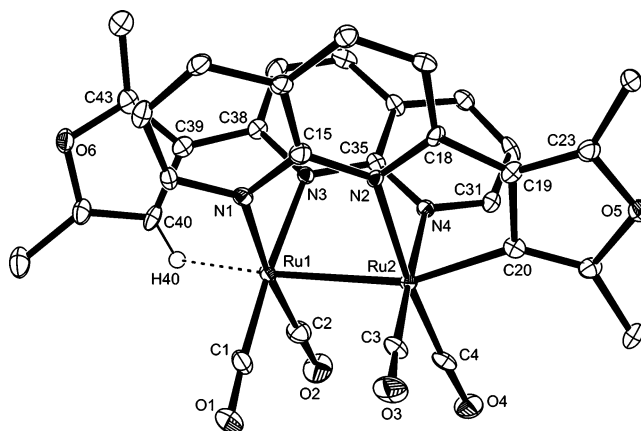


Figure 2. ORTEP diagram (50% probability thermal ellipsoids) of the cationic unit $[Ru_2(Me_2fuNP)(C_4OMe_2-NP)(CO)_4]^+$ in compound **2** with important atoms labeled. Hydrogen atoms, except for the agostic hydrogen, are omitted for the sake of clarity.

(1)° are marginally shorter than those observed in compound **1**. The N3–C38–C39–C40 torsion angle of 37.93(1)° is significantly shorter than the corresponding angle in **1**. In ¹H NMR, the agostic hydrogen appears as a doublet at δ 9.35 ppm, in addition to two sets of aromatic signals for the two ligands.

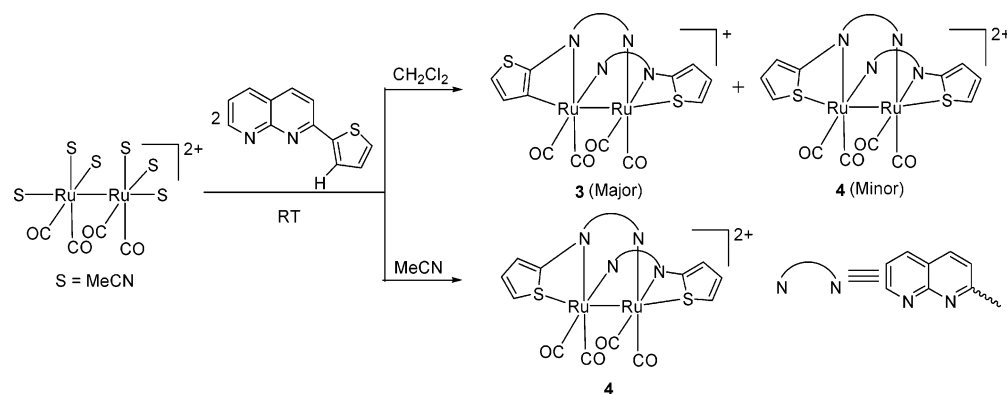
In both compounds **1** and **2**, metal insertion into the C–H bond occurs at one of the ligands, while the second ligand is engaged in an agostic interaction. Prolonged heating in refluxing

Table 1. Relevant Metrical Parameters of Compounds 1–3

	1	2	3
Bond Distances (Å)			
Ru–Ru	2.6924(9)	2.6875(6)	2.6938(7)
Ru–C(ax)	2.074(5)	2.066(5)	2.100(6)
Ru–S(ax)			2.5864(17)
Ru–N(eq)	2.163(4), 2.161(4), 2.143(4), 2.218(4)	2.162(4), 2.177(4), 2.184(4), 2.185(4)	2.175(5), 2.170(5), 2.161(5), 2.188(5)
Ru–C(CO)	1.854(6)–1.864(5)	1.854(6)–1.857(5)	1.848(7)–1.879(7)
Bond Angles (deg)			
Ru–Ru–C(ax)	160.52(14)	159.48(14)	158.7(2)
Ru–Ru–S(ax)			163.74(4)
Ru–Ru–N(eq)	84.61(11), 85.92(11), 83.62(11), 82.15(11)	86.35(11), 84.75(10), 82.26(11), 82.57(11)	82.20(13), 83.10(13), 84.15(13), 85.38(13)
N–Ru–N	87.18(15), 88.11(15)	83.07(15), 86.29(15)	86.62(19), 84.43(19)
C–Ru–N	79.21(18), 88.10(17)	79.03(17), 87.85(17)	78.8(2), 86.4(2)
C(ax)–Ru–C(CO)	91.4(2), 95.1(2)	89.3(2), 95.9(2)	93.1(3), 97.7(3)
Torsion Angles (deg)			
N–C–C–C ^a	7.8(7)	3.5(6)	5.3(10)

^a Angle between the planes of NP and the cyclometalated aromatic ring.

Scheme 2



dichloroethane does not lead to a second metalation, and only the monometalated product was identified from the NMR and absorption spectra (vide infra).

The thienyl appendage in thNP offers two possibilities: axial S coordination to the metal and metal insertion into the ortho C–H bond. In dichloromethane, the red cyclometalated compound $[\text{Ru}_2(\text{thNP})(\text{C}_4\text{H}_2\text{S-NP})(\text{CO})_4][\text{BF}_4]$ (**3**) was isolated as the major product, in addition to a small amount of the yellow $[\text{Ru}_2(\text{thNP})_2(\text{CO})_4][\text{BF}_4]_2$ (**4**). In acetonitrile, however, compound **4** was obtained exclusively, with no trace of **3** (Scheme 2). This result shows that noncoordinating solvents are preferred over coordinating solvents for the C–H bond activation. The ortho metalation of one thNP over the potential S coordination was unambiguously confirmed from the X-ray structure of **3** (Figure 3).

The second thNP prefers axial S ligation and not C–H coordination to ruthenium. The relevant metrical parameters are $\text{Ru1}–\text{Ru2} = 2.694(1)$ Å, $\text{Ru2}–\text{C20} = 2.100(6)$ Å, and $\text{Ru1}–\text{Ru2}–\text{C20} = 158.7(2)^\circ$ (Table 1). The torsion angle ($\text{N3}–\text{C38}–\text{C39}–\text{S2}$) between the S-ligated thienyl and NP planes is $35.2(8)^\circ$. The corresponding value for the ortho-metalated thNP is $5.3(10)^\circ$. The ^1H NMR of compound **3** displays two distinct sets of aromatic signals for the two ligands. The identical environments of the two ligands around the dimetal unit in compound **4** are reflected in the ^1H NMR spectrum, exhibiting one set of aromatic signals. The NMR and UV–vis absorption data suggest a structure similar to that of $[\text{Ru}_2(\text{fuNP})_2(\text{CO})_4][\text{BF}_4]_2$ (fuNP = 2-(2-furyl)-1,8-naphthyridine), reported earlier.⁵ Both of the thNP ligands in compound **4** are engaged axially through S coordination (Scheme 2).

Agostic Compounds with the $[\text{Rh}_2]^{4+}$ Unit. The successful cleaving of the C–H bond by the $[\text{Ru}_2(\text{CO})_4]^{2+}$ core prompted us to use the isoelectronic $[\text{Rh}_2]^{4+}$ precursor. The weakening of the C–H bond at axial site of the $[\text{Rh}_2]^{4+}$ unit was suggested from the NMR data.⁸ Reaction of phNP with $\text{Rh}_2(\text{OAc})_4$ in refluxing 1,2-dichloroethane and subsequent crystallization in dichloromethane resulted in the formation of $[\text{Rh}_2(\text{OAc})_3(\text{phNP})\text{Cl}]$ (**5**), incorporating only one phNP in the dirhodium core. The molecular structure of **5**, depicted in Figure 4, provides

evidence for the agostic configuration of the C–H bond to the dirhodium unit ($\text{Rh2}–\text{H20} = 2.462$ Å (calculated), $\text{Rh2}–\text{C20} = 2.822(3)$ Å, $\text{Rh2}–\text{H20}–\text{C20} = 102.4(2)^\circ$ and $\text{N2}–\text{C18}–\text{C19}–\text{C20} = 47.0(5)^\circ$). The $\text{Rh1}–\text{Rh2}$ and the $\text{Rh1}–\text{C11}$ distances are 2.3947(4) and 2.4593(9) Å, respectively (Table 2).

The use of $[\text{Rh}_2(\text{OAc})_2(\text{MeCN})_6][\text{BF}_4]_2$, involving the labile ligands MeCN, did not result in the expected product $[\text{Rh}_2(\text{phNP})_2(\text{OAc})_2][\text{BF}_4]_2$. The isolated product is $[\text{Rh}_2(\text{phNP})(\eta^1-$

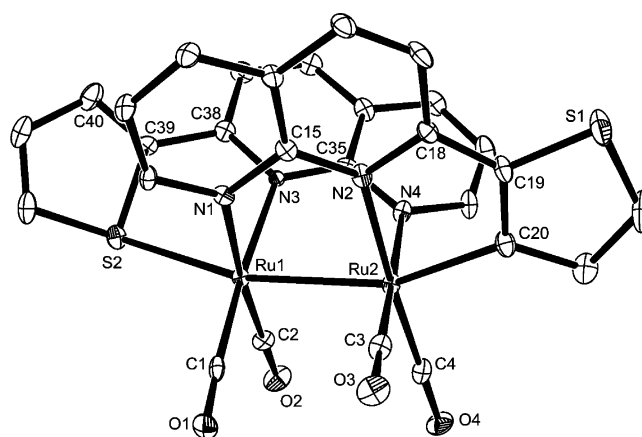


Figure 3. ORTEP diagram (30% probability thermal ellipsoids) of the cationic unit $[\text{Ru}_2(\text{thNP})(\text{C}_4\text{H}_2\text{S-NP})(\text{CO})_4]^+$ in compound **3** with important atoms labeled. Hydrogen atoms are omitted for the sake of clarity.

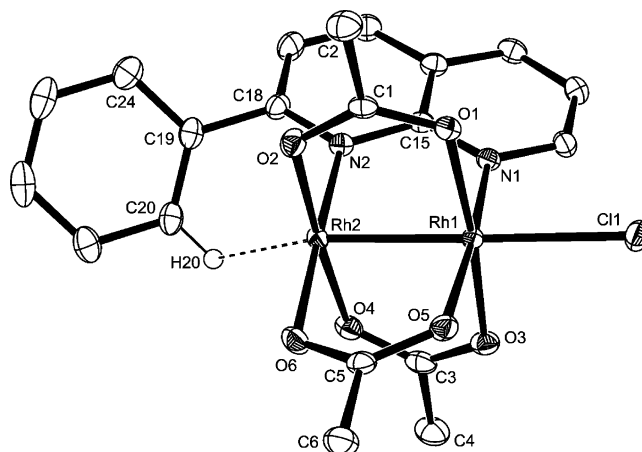


Figure 4. ORTEP diagram (50% probability thermal ellipsoids) of the molecular structure of $[\text{Rh}_2(\text{phNP})(\text{OAc})_3\text{Cl}]$ (**5**) with important atoms labeled. Hydrogen atoms, except for the agostic hydrogen, are omitted for the sake of clarity.

(6) (a) Tenorio, M. J.; Mereiter, K.; Puerta, M. C.; Valerga, P. *J. Am. Chem. Soc.* **2000**, *122*, 11230. (b) Baratta, W.; Herdtweck, E.; Rigo, P. *Angew. Chem., Int. Ed.* **1999**, *38*, 1629. (c) Huang, D.; Streib, W. E.; Bollinger, J. C.; Caulton, K. G.; Winter, R. F.; Scheiring, T. *J. Am. Chem. Soc.* **1999**, *121*, 8087. (d) Crabtree, R. H. *Angew. Chem., Int. Ed. Engl.* **1993**, *32*, 789. (e) Brookhart, M.; Green, M. L. H.; Wong, L. L. *Prog. Inorg. Chem.* **1988**, *36*, 1.

(7) Toner, A. J.; Gründemann, S.; Clot, E.; Limbach, H.-H.; Donnadieu, B.; Sabo-Etienne, S.; Chaudret, B. *J. Am. Chem. Soc.* **2000**, *122*, 6777.

(8) Thummel, R. P.; Lefoulon, F.; Williamson, D.; Chavan, M. *Inorg. Chem.* **1986**, *25*, 1675.

Table 2. Relevant Metrical Parameters of Compounds 5 and 7

	5	7
Bond Distances (Å)		
Rh–Rh	2.3947(4)	2.4615(9)
Rh–N(ax)		2.199(6)
Rh–Cl(ax)	2.4593(9)	
Rh–N(eq)	2.040(3), 2.010(3)	2.044(5), 1.975(6), 2.002(6), 1.985(6)
Rh–O(eq)	2.033(2)–2.049(2)	2.014(4)–2.042(5)
Bond Angles (deg)		
Rh–Rh–N(ax)		169.51(15)
Rh–Rh–Cl(ax)	176.81(2)	
Rh–Rh–N(eq)	88.14(8), 89.69(8)	93.89(17), 88.63(16), 100.45(18), 89.3(2)
N–Rh–N		90.4(2), 91.3(2)
O–Rh–N(eq)	89.63(11), 92.09(10)	88.7(2)–91.2(2), 173.9(2)–178.7(2)

phNP)(OAc)₂(CH₃CN)₂][BF₄]₂ (**6**). The ¹H NMR of compound **6** exhibits two sets of signals for the bridging and axially coordinated phNP and shows no C–H activation but a substantial weakening of the aryl C–H bond. The doublet at δ 10.18 ppm indicates an agostic hydrogen lying close to the dirhodium internuclear axis.⁸ An analogous agostic compound, [Rh₂(nplNP)(η¹-nplNP)(OAc)₂(CH₃CN)₂][BF₄]₂ (**7**), has been synthesized from the reaction of [Rh₂(OAc)₂(MeCN)₆][BF₄]₂ and nplNP. The structure has been determined by X-ray crystallography (Figure 5), and the important metrical parameters are given in Table 2. In this compound, the dirhodium unit possesses one nplNP ligand bridging the dimetal core, with a second nplNP ligand acting as a monodentate axial ligand involving one of the N atoms of the NP unit. The ortho “H” atom of the naphthyl appendage of the bridging NP is in the vicinity of Rh2. The relevant structural parameters are Rh1–Rh2 = 2.4615(9) Å, Rh2–H20 = 2.499 Å (calculated), Rh2–C20 = 2.654(9) Å, and Rh2–H20–C20 = 88.7(1)°. The N2–C18–C19–C20 torsional angle of 48.9(11)° reveals an agostic configuration of the naphthyl C–H bond with the [Rh₂]⁴⁺ core. The corresponding angle of the axially coordinating nplNP is 1.9(10)°. The methyl protons of the two coordinated acetonitriles display four resonances with intensities 2:1:1:2. Three of the resonances are shifted upfield, and this shift is attributed in large part to the

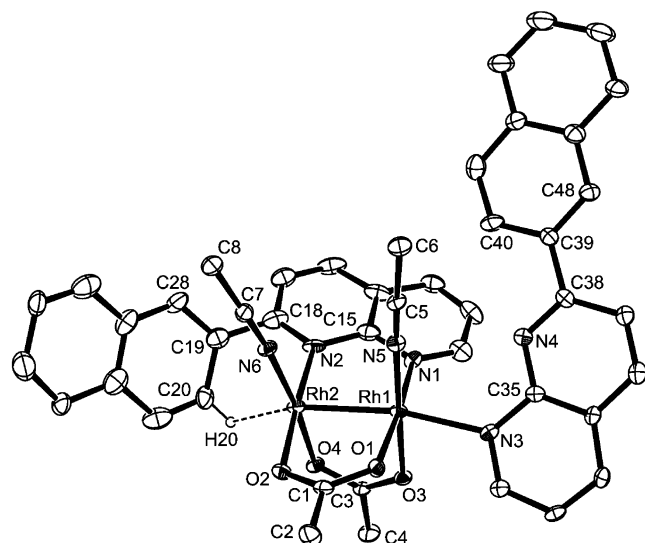


Figure 5. ORTEP diagram (30% probability thermal ellipsoids) of the cationic unit $[Rh_2(nplNP)(\eta^1-nplNP)(OAc)_2(CH_3CN)_2]^{2+}$ in compound **7** with important atoms labeled. Hydrogen atoms, except for the agostic hydrogen, are omitted for the sake of clarity.

Table 3. Absorption and Emission Spectral Data^a for Compounds 1–7 at Room Temperature

compd	absorption λ_{max} , nm (log ϵ^b)			emission λ_{max} , nm	
1	248 (4.55)	324 (4.52)	434 (3.78)		415
2	252 (4.34)	338 (4.12)	420 (3.79)	525 (3.26)	435
3	272 (4.67)	342 (4.58)	362 (4.59)	505 (3.46)	406, 472
4^c	264 (4.43)	342 (4.36)	354 (4.36)		410
5	231 (4.37)	284 (4.46)	314 (4.06)	484 (3.57)	378
6	230 (4.74)	264 (4.71)	310 (4.66)	342 (4.65)	392
7	232 (4.87)	320 (4.72)	392 (sh)		385

^a Absorption and emission studies were done in dichloromethane unless otherwise noted. ^b ϵ is given in units of $cm^3 mol^{-1} cm^{-1}$. ^c Absorption and emission studies were done in acetonitrile.

effects of the aromatic ring current of the NP ligand.⁹ A careful examination of the X-ray structure reveals the nonequivalent interactions of the methyl protons with the NP rings. Similar behavior is also noted for compound **6**.

The agostic protons in dirhodium compounds exhibit larger downfield shifts compared to the $[Ru_2]^{2+}$ compounds reported herein. Metalation, however, was not accomplished, even after prolonged heating of compounds **5–7** in refluxing 1,2-dichloroethane.

Absorption and Emission Spectra. The reactions described above provide access to new types of cyclometalated compounds that contain a metal–metal-bonded system. The absorption data of the compounds are compiled in Table 3. The absorption spectra of the compounds **1–4** display strong bands in the far-UV region at 248, 252, 272, and 264 nm, respectively, assigned to dimetal-based $\pi^* \rightarrow \sigma^*$ transitions.¹⁰ The lower energy transitions in the region 320–420 nm are likely to be from $[Ru_2]^{2+}$ bond orbitals to empty π^* orbitals largely based on the ligands. These values are comparable to those observed in $[Ru_2(CO)_4L_2]^{2+}$, where L denotes NP-based ligands with furyl, thiazolyl, and pyridyl appendages at the 2-position.⁵ The most salient feature for the ortho-metallated compounds **1–3** is the appearance of weak and broad absorption peaks at 434, 525, and 505 nm, respectively, which are apparently absent in similar compounds but do not contain an Ru–C bond.¹¹ These are assigned to MLCT transitions typical of the cyclometalated diruthenium compounds. The lack of a similar low-energy band in **4** confirms that the thienyl units are not ortho-metallated but, rather, coordinated axially through the S centers.

The absorption spectra of compounds **5–7** exhibit multiple strong absorptions in the range of 230–400 nm. These are assigned as metal-based $\pi^* \rightarrow \sigma^*$ and MLCT transitions associated with the NP ligands. Compound **5**, which bears an axial chloride, exhibits an additional low-energy absorption at 484 nm. The UV–vis absorptions of $[Rh_2]^{4+}$ complexes are known to vary widely with the axial donors.^{10,12}

The emission spectra of cyclometalated compounds containing C[^]N-coordinating ligands are of considerable interest.¹³ All of the compounds are luminescent in degassed solution at room temperature, and the emission data are provided in Table 3. Excitation wavelengths are selected on the basis of absorption

(9) Tikkanen, W. R.; Binamira-Soriaga, E.; Kaska, W. C.; Ford, P. C. *Inorg. Chem.* **1984**, *23*, 141.

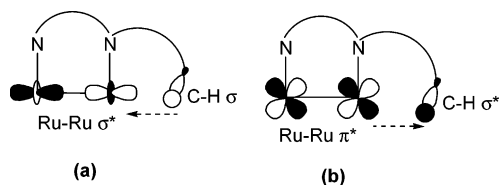
(10) Martin, D. S., Jr.; Webb, T. R.; Robbins, G. A.; Fanwick, P. E. *Inorg. Chem.* **1979**, *18*, 475.

(11) Li, H.-C.; Chou, P.-T.; Hu, Y.-H.; Cheng, Y.-M.; Liu, R.-S. *Organometallics* **2005**, *24*, 1329.

(12) (a) Clark, R. J. H.; Hempleman, A. J. *Inorg. Chem.* **1989**, *28*, 746. (b) Cotton, F. A.; Felthouse, T. R. *Inorg. Chem.* **1981**, *20*, 584.

(13) (a) Dixon, I. M.; Collin, J.-P.; Flamigni, L.; Encinas, S.; Barigelletti, F. *Chem. Soc., Rev.* **2000**, *29*, 385. (b) Balzani, V.; Juris, A.; Venturi, M.; Campagna, S.; Serroni, S. *Chem. Rev.* **1996**, *96*, 759.

Scheme 3



spectra. The diruthenium cyclometalated compounds **1** and **2** display broad emissions centered at 415 and 435 nm, respectively. The lowest energy emission of **3** appears at 472 nm, in addition to a peak at 406 nm. The diruthenium compound **4** shows emission at 410 nm. It should be noted here that compound **3** involves C-ligated and S-ligated thienyl units at axial sites of the Ru–Ru core, whereas compound **4** contains only S-ligated thienyls. The electronic transitions responsible for luminescence in these complexes have been assigned to a mixture of metal-to-ligand charge-transfer (MLCT) and $^3(\pi-\pi^*)$ ligand states.¹⁴ The dirhodium compounds exhibit emissions at much higher energy in the region of 378–392 nm.

Possible Reaction Pathway. The agostic configuration of the C–H bond at the axial site of the dimetal core, as reflected in the X-ray structures of the compounds, strongly suggests that the metalation proceeds through the intermediacy of the “agostic complex”. The deprotonation of the agostic intermediate and the elimination of HBF_4 during metalation most likely occurs via the electrophilic pathway recently proposed by Milstein.¹⁵ The coordinatively saturated Ru center does not support a possible “oxidative addition/reductive elimination” mechanism.^{1f}

We offer a theoretical framework based on orbital interactions to explain the propensity of the $[\text{Ru}_2(\text{CO})_4]^{2+}$ core to activate the C–H bond. The DFT calculation on the $[\text{Ru}_2(3\text{-MeNP})_2(\text{CO})_4]^{2+}$ unit (3-MeNP = 3-methyl-1,8-naphthyridine) confirms that the LUMO is a metal-based σ^* orbital resulting from the antibonding interaction of the two d_z^2 orbitals and the HOMO and HOMO-1 are closely spaced Ru–Ru π^* orbitals originating from out-of-phase $d_{xz}-d_{yz}$ and $d_{yz}-d_{xz}$ interactions.⁵ The C–H bond at the site trans to the Ru–Ru bond donates the bonding electron pair to the Ru–Ru σ^* LUMO, and the back-donation occurs from the filled Ru–Ru π^* to the C–H σ^* orbital, as depicted in Scheme 3. The combination of these two interactions results in C–H bond cleavage. The extent of back-donation from the high-energy Ru–Ru $d\pi^*$ orbital is anticipated to be higher in comparison to the electron flow from the “nonbonding” $d\pi$ orbital of the monometal species. This explains the advantage of the $[\text{Ru}-\text{Ru}]^{2+}$ unit over mononuclear ruthenium complexes, which often require high thermal energy for cyclometalation.¹⁶ Notably, the subsequent metalation of the second ligand does not occur, despite the presence of another Ru–Ru $d\pi^*$ orbital fully available for back-donation. The reason probably lies with the fact that the Ru–Ru σ^* orbital is no longer a good acceptor

orbital to accommodate electron density from the second C–H σ bond once the first metalation is achieved.¹⁷ The inability of the isoelectronic $[\text{Rh}_2(\text{OAc})_2]^{2+}$ core to cleave the C–H bond is attributed to the higher positive charge on Rh, resulting in weak back-bonding from the dirhodium unit to the C–H σ^* orbital.

Conclusion

The present work endorses Chisholm’s assertion¹⁸ with regard to the scope of the dimetal unit. The highlight of this work is the room-temperature cleavage of the aromatic C–H bond by the $[\text{Ru}_2(\text{CO})_4]^{2+}$ core in dichloromethane, leading to cyclometalated compounds containing an Ru–Ru single bond. The metal insertion into the C–H bond occurs at one of the aryl units located at a site trans to the Ru–Ru bond. The second aryl C–H is engaged in an agostic interaction. Noncoordinating solvents are preferred over acetonitrile for C–H bond activation. The $[\text{Rh}_2]^{4+}$ unit containing acetates as ancillary ligands provides only the agostic compounds. The agostic interactions recognized in the isolated compounds offer insight into the mechanism of these reactions. The electronic basis for the advantage of the dimetal unit over its monometal congener is suggested. It is our expectation that this work will open up a new area of organometallic chemistry that employs metal–metal-bonded dimetal units.

Experimental Section

General Methods. All reactions with metal complexes were carried out under an atmosphere of purified nitrogen using standard Schlenk-vessel and vacuum line techniques. Glasswares were flame-dried under vacuum prior to use. Solvents were dried by conventional methods, distilled over nitrogen, and deoxygenated prior to use.¹⁹ $\text{RuCl}_3 \cdot n\text{H}_2\text{O}$ (39% Ru) was purchased from Arora Matthey, Calcutta, India. The compound $[\text{Ru}_2(\text{CO})_4(\text{CH}_3\text{CN})_6][\text{BF}_4]_2$ was synthesized by following a procedure similar to the synthesis of $[\text{Ru}_2(\text{CO})_4(\text{CH}_3\text{CN})_6][\text{PF}_6]_2$.²⁰ The compounds $\text{Rh}_2(\text{OAc})_4$ ²¹ and $[\text{Rh}_2(\text{OAc})_2(\text{CH}_3\text{CN})_6][\text{BF}_4]_2$ ²² were synthesized according to the literature procedures. The ligands phNP, Me₂fuNP, thNP, and nplNP were prepared by the Friedlander condensation of 2-aminonicotinaldehyde with the corresponding acyl derivatives.²³ Synthetic procedures and NMR data for the ligands are provided as Supporting Information. Infrared spectra were recorded in the range 4000–400 cm^{-1} on a Vertex 70 Bruker spectrophotometer on KBr pellets. ¹H NMR spectra were obtained on a JEOL JNM-LA 400 MHz spectrometer. ¹H NMR chemical shifts were referenced to the residual hydrogen signal of the deuterated solvents. Elemental analyses were performed on a Thermoquest EA1110 CHNS/O analyzer. Electronic absorptions were measured on a Perkin-Elmer Lambda-20 spectrophotometer. Emission spectral data at room temperature were obtained with a Perkin-Elmer LS 50B lumines-

(14) (a) Wilkinson, A. J.; Goeta, A. E.; Foster, C. E.; Williams, J. A. *Inorg. Chem.* **2001**, *43*, 6513. (b) Lamansky, S.; Djurovich, P.; Murphy, D.; Abdel-Razzaq, F.; Lee, H.-E.; Adachi, C.; Burrows, P. E.; Forrest, S. R.; Thompson, M. E. *J. Am. Chem. Soc.* **2001**, *123*, 4304. (c) Sprouse, S.; King, K. A.; Spellane, P. J.; Watts, R. J. *J. Am. Chem. Soc.* **1984**, *106*, 6647.

(15) Vignalok, A.; Uzan, O.; Shimon, L. J. W.; Ben-David, Y.; Martin, J. M. L.; Milstein, D. *J. Am. Chem. Soc.* **1998**, *120*, 12539.

(16) (a) Gupta, P.; Dutta, S.; Basuli, F.; Peng, S.; Lee, G.; Bhattacharya, S. *Inorg. Chem.* **2006**, *45*, 460. (b) Pearson, P.; Kepert, C. M.; Deacon, G. B.; Spiccia, L.; Warden, A. C.; Skelton, B. W.; White, A. H. *Inorg. Chem.* **2004**, *43*, 683. (c) Hadadzadeh, H.; DeRosa, M. C.; Yap, G. P. A.; Rezvani, A. R.; Crutchley, R. J. *Inorg. Chem.* **2002**, *41*, 6521. (d) Ryabov, A. D.; Sukharev, V. S.; Alexandrova, L.; Lagadec, R. L.; Pfeffer, M. *Inorg. Chem.* **2001**, *40*, 6529. (e) Bonnefous, C.; Chouai, A.; Thummel, R. P. *Inorg. Chem.* **2001**, *40*, 5851.

(17) The destabilization of a metal–metal σ^* orbital due to axial coordination has been reported. See: Norman, J. G., Jr.; Kolari, H. J. *J. Am. Chem. Soc.* **1978**, *100*, 791.

(18) Chisholm, M. H. Anything One Can Do, Two Can Do, Too - and It’s More Interesting. *ACS Symp. Ser.* **1981**, No. 155, 17.

(19) Perrin, D. D.; Armarego, W. L. F.; Perrin, D. R. *Purification of Laboratory Chemicals*, 2nd ed.; Pergamon Press: 1980.

(20) Klemperer, W. J.; Zhong, B. *Inorg. Chem.* **1993**, *32*, 5821.

(21) Rempel, G. A.; Smith, L. H.; Wilkinson, G. *Inorg. Synth.* **1972**, *13*, 90.

(22) Pimblett, G.; Garner, C. D.; Clegg, W. *J. Chem. Soc., Dalton Trans.* **1986**, 1257.

(23) (a) Reddy, K. V.; Mogilaiah, K.; Sreenivasulu, B. *J. Indian Chem. Soc.* **1986**, *63*, 443. (b) Thummel, R. P.; Lefoulon, F.; Cantu, D.; Mahadevan, R. *J. Org. Chem.* **1984**, *49*, 2208. (c) Majewicz, T. C.; Caluwe, P. *J. Org. Chem.* **1974**, *39*, 720. (d) Hawes, E. M.; Wibberley, D. G. *J. Chem. Soc.* **1966**, 315.

Table 4. Crystallographic Data and Refinement Parameters for Compounds 1–3, 5 and 7

	1·2CH ₂ Cl ₂	2·CH ₂ Cl ₂	3	5·CH ₂ Cl ₂	7·3CH ₂ Cl ₂
empirical formula	C ₃₄ H ₂₃ BCl ₄ F ₄ - N ₄ O ₄ Ru ₂	C ₃₃ H ₂₃ BCl ₄ F ₄ - N ₄ O ₆ Ru ₂	C ₂₈ H ₁₅ BF ₄ N ₄ - O ₄ Ru ₂ S ₂	C ₂₁ H ₁₉ Cl ₃ N ₂ - O ₆ Rh ₂	C ₄₇ H ₄₂ B ₂ Cl ₆ F ₈ - N ₆ O ₄ Rh ₂
formula wt	982.31	933.42	824.51	707.55	1347.01
cryst syst	triclinic	orthorhombic	monoclinic	monoclinic	monoclinic
space group	<i>P</i> $\bar{1}$	<i>Pbca</i>	<i>P</i> 2 ₁ / <i>c</i>	<i>P</i> 2 ₁ / <i>c</i>	<i>P</i> 2 ₁ / <i>c</i>
<i>a</i> , Å	8.7967(18)	11.6387(7)	10.9954(14)	16.2584(8)	11.6974(17)
<i>b</i> , Å	13.448(3)	20.9611(13)	20.666(3)	8.3000(4)	22.563(3)
<i>c</i> , Å	15.832(3)	28.5005(17)	15.687(2)	19.3585(10)	21.130(3)
α , deg	86.44(3)				
β , deg	88.89(3)		106.961(2)	109.4310(10)	95.951(3)
γ , deg	71.43(3)				
<i>V</i> , Å ³	1771.9(6)	6953.0(7)	3409.5(8)	2463.5(2)	5546.8(14)
<i>Z</i>	2	8	4	4	4
ρ_{calcd} , g cm ⁻³	1.841	1.783	1.606	1.908	1.613
μ , mm ⁻¹	1.221	1.095	1.067	1.705	0.958
<i>F</i> (000)	968	3696	1616	1392	2688
no. of rflns					
collected	10 218	38 819	18 812	13 893	36 413
indep	7045	7092	6945	5015	13 579
obsd (<i>I</i> > 2 σ (<i>I</i>))	5354	6130	4689	4598	8697
no. of variables	478	468	401	304	680
goodness of fit	1.000	1.241	0.961	1.065	1.067
final <i>R</i> indices (<i>I</i> > 2 σ (<i>I</i>)) ^a					
<i>R</i> 1	0.0496	0.0597	0.0610	0.0355	0.0866
<i>wR</i> 2	0.1095	0.1120	0.1411	0.0928	0.1777
<i>R</i> indices (all data) ^a					
<i>R</i> 1	0.0724	0.0729	0.0924	0.0386	0.1353
<i>wR</i> 2	0.1208	0.1166	0.1543	0.0949	0.2016

^a *R*1 = $\sum||F_o| - |F_c||/\sum|F_o|$ with $F_o^2 > 2\sigma(F_o^2)$. *wR*2 = $[\sum w(|F_o|^2 - |F_c|^2)|^2/\sum|F_o|^2]^2$.

cence spectrometer. Degassed dichloromethane or acetonitrile solvent was used for the emission measurements in the concentration range of 10⁻⁵–10⁻⁶ M.

Synthesis of [Ru₂(phNP)(C₄H₄-NP)(CO)₄][BF₄] (1). A dichloromethane solution (10 mL) of phNP (19 mg, 0.092 mmol) was added dropwise to a dichloromethane solution (15 mL) of [Ru₂(CO)₄(MeCN)₆][BF₄]₂ (30 mg, 0.041 mmol), and the solution was stirred for 4 h at room temperature. The red solution was subsequently concentrated, and ether was added to induce precipitation. The red solid was collected by filtration, washed with ether, and dried under vacuum. Yield: 29 mg (87%). ¹H NMR (CD₂Cl₂, δ): 9.29 (dd, 1H), 8.45 (d, 1H), 8.42 (dd, 1H), 8.31–8.18 (m, 5H), 8.04 (t, 1H), 7.96 (d, 1H), 7.93 (m, 2H), 7.76 (m, 2H), 7.55 (td, 1H), 7.50 (q, 1H), 7.25 (m, 1H), 7.09 (m, 1H), 6.99 (d, 1H). ¹³C-{¹H} NMR (CD₂Cl₂, δ): 207.4, 203.8, 200.3, 181.2, 167, 161.2, 156, 134.2, 132.3, 130, 129, 125.1, 124, 122.7, 121.4. IR (KBr, cm⁻¹): ν (CO) 2025, 1945; ν (BF₄⁻) 1058. Anal. Calcd for C₃₂H₁₉N₄O₄BF₄Ru₂: C, 47.31; H, 2.36; N, 6.90. Found: C, 47.16; H, 2.39; N, 7.04.

Synthesis of [Ru₂(Me₂fuNP)(C₄OMe₂-NP)(CO)₄][BF₄] (2). The reaction of [Ru₂(CO)₄(MeCN)₆][BF₄]₂ (28 mg, 0.038 mmol) and Me₂fuNP (20 mg, 0.089 mmol) was carried out by following a procedure similar to that described in the synthesis of complex 1. Yield: 30 mg (93%). ¹H NMR (CD₂Cl₂, δ): 9.35 (d, 1H), 8.49 (m, 2H), 8.32 (1H), 8.14 (1H), 7.90 (s, 1H), 7.70 (m, 2H), 7.58 (m, 2H), 7.37 (t, 1H), 2.73 (s, 6H), 2.61 (s, 3H), 1.97 (s, 3H). IR (KBr, cm⁻¹): ν (CO) 2030, 1954; ν (BF₄⁻) 1064. Anal. Calcd for C₃₂H₂₃N₄O₆BF₄Ru₂: C, 45.30; H, 2.73; N, 6.60. Found: C, 45.02; H, 2.79; N, 6.72.

Synthesis of [Ru₂(thNP)(C₄H₂S-NP)(CO)₄][BF₄] (3) and [Ru₂(thNP)₂(CO)₄][BF₄]₂ (4). A dichloromethane solution (10 mL) of thNP (36 mg, 0.169 mmol) was added dropwise to a dichloromethane solution (15 mL) of [Ru₂(CO)₄(MeCN)₆][BF₄]₂ (55 mg, 0.075 mmol), and the solution was stirred for 4 h at room temperature. A small amount of bright yellow residue was formed, which was separated by filtration through a filter-paper-stripped cannula. The red filtrate was concentrated, and diethyl ether was added to induce precipitation. The red residue was washed with diethyl ether and dried under vacuum. The red product was

characterized as the cyclometalated complex [Ru₂(thNP)(C₄H₂S-NP)(CO)₄][BF₄] (3). Yield: 42 mg (68%). ¹H NMR (CD₂Cl₂, δ): 9.07 (dd, 1H), 8.49 (m, 2H), 8.16 (dd, 1H), 8.03 (m, 3H), 7.90 (dd, 1H), 7.86 (d, 1H), 7.73 (m, 1H), 7.56 (dd, 1H), 7.53 (d, 1H), 7.57 (q, 1H), 7.18 (dd, 1H), 7.10 (q, 1H). IR (KBr, cm⁻¹): ν (CO) 2028, 1956; ν (BF₄⁻) 1060. Anal. Calcd for C₂₈H₁₅N₄S₂O₄BF₄Ru₂: C, 40.79; H, 1.83; N, 6.80; S, 7.78. Found: C, 41.10; H, 1.98; N, 6.94; S, 7.55.

The bright yellow product was characterized as [Ru₂(thNP)₂(CO)₄][BF₄]₂ (4). Yield: 14 mg (20%). ¹H NMR (CD₃CN, δ): 8.58 (d, 2H), 8.52 (d, 2H), 8.14 (d, 2H), 8.06 (d, 2H), 7.88 (d, 2H), 7.77 (m, 2H), 7.54 (d, 2H), 7.28 (d, 2H). IR (KBr, cm⁻¹): ν (CO) 2061, 1985; ν (BF₄⁻) 1068. Anal. Calcd for C₂₈H₁₆N₄S₂O₄B₂F₈Ru₂: C, 36.86; H, 1.77; N, 6.14; S, 7.03. Found: C, 36.63; H, 1.87; N, 6.28; S, 6.95.

[Ru₂(thNP)₂(CO)₄][BF₄]₂ (4) was isolated in 86% yield when the reaction was carried out in acetonitrile by following a procedure similar to that described for compound 3.

Synthesis of [Rh₂(phNP)(OAc)₃Cl] (5). A sample of [Rh₂(OAc)₄] (35 mg, 0.079 mmol) was treated with 36 mg (0.175 mmol) of phNP in 15 mL of 1,2-dichloroethane and refluxed for 12 h. The red solution was concentrated, and ether was added to induce precipitation. The red residue obtained was washed with ether and dried under vacuum. Yield: 42 mg (85%). ¹H NMR (CDCl₃, δ): 11.38 (d, 1H), 8.61 (d, 2H), 8.32 (q, 2H), 8.08 (2H), 7.92 (dd, 2H), 7.75 (t, 1H), 2.16 (s, 3H), 1.68 (s, 3H), 1.23 (s, 3H). IR (KBr, cm⁻¹): ν (OAc⁻) 1604, 1552, 1434. Anal. Calcd for C₂₀H₁₉N₂O₆ClRh₂: C, 38.46; H, 3.07; N, 4.48. Found: C, 38.68; H, 3.12; N, 4.36.

Synthesis of [Rh₂(phNP)(η^1 -phNP)(OAc)₂(CH₃CN)₂][BF₄]₂ (6). A sample of [Rh₂(OAc)₂(MeCN)₆][BF₄]₂ (38 mg, 0.051 mmol) was treated with 25 mg (0.116 mmol) of phNP in 15 mL of 1,2-dichloroethane and refluxed for 12 h. The red solution was concentrated, and ether was added to induce precipitation. The red residue obtained was washed with ether and dried under vacuum. Yield: 42 mg (83%). ¹H NMR (CDCl₃, δ): 10.18 (d, 1H), 8.58 (dd, 2H), 8.72 (dd, 1H), 8.41 (m, 2H), 8.33 (td, H), 8.25 (d, 2H), 8.17 (d, H), 7.99 (m, 6H), 7.57 (d, H), 7.42 (m, 3H), 2.91 (s, 1H), 2.14 (t, 6H), 2.05 (s, 1H), 2.02 (s, 1H), 1.24 (br, 1H), 0.85 (m,

2H). IR (KBr, cm^{-1}): $\nu(\text{OAc}^-)$ 1609, 1556, 1444; $\nu(\text{BF}_4^-)$ 1058. Anal. Calcd for $\text{C}_{36}\text{H}_{32}\text{N}_6\text{O}_4\text{B}_2\text{F}_8\text{Rh}_2$: C, 43.58; H, 3.25; N, 8.47. Found: C, 43.36; H, 3.37; N, 8.61.

Synthesis of $[\text{Rh}_2(\text{npINP})(\eta^1\text{-npINP})(\text{OAc})_2(\text{CH}_3\text{CN})_2][\text{BF}_4]_2$ (7). The reaction of $[\text{Rh}_2(\text{OAc})_2(\text{MeCN})_6][\text{BF}_4]_2$ (31 mg, 0.042 mmol) and 25 mg (0.097 mmol) of npINP in 15 mL of 1,2-dichloroethane was carried out by following a procedure similar to that described in the synthesis of complex **6**. Yield: 38 mg (84%). ^1H NMR (CDCl_3 , δ): 10.21 (d, 1H), 8.74 (d, 1H), 8.33 (dd, 2H), 8.26 (d, 2H), 7.92 (q, 2H), 7.82 (td, 4H), 7.67 (d, 1H), 7.45 (m, 4H), 7.37 (m, 2H), 7.23 (m, 5H), 2.95 (s, 2H), 2.23 (s, 6H), 1.98 (s, 1H), 1.24 (br, 1H), 0.84 (m, 2H). IR (KBr, cm^{-1}): $\nu(\text{OAc}^-)$ 1610, 1557, 1442; $\nu(\text{BF}_4^-)$ 1058. Anal. Calcd for $\text{C}_{44}\text{H}_{36}\text{N}_6\text{O}_4\text{B}_2\text{F}_8\text{Rh}_2$: C, 48.39; H, 3.32; N, 7.69. Found: C, 48.12; H, 3.49; N, 7.57.

X-ray Data Collections and Refinement. The red single crystals of **1–3**, **5**, and **7** were harvested by layering petroleum ether onto the dichloromethane solutions of the compounds in 8 mm o.d. glass tubes. Single-crystal X-ray structural studies were performed on a CCD Bruker SMART APEX diffractometer equipped with an Oxford Instruments low-temperature attachment. Data were collected at 100(2) K using graphite-monochromated Mo $\text{K}\alpha$ radiation ($\lambda_\alpha = 0.71073 \text{ \AA}$). The frames were indexed, integrated, and scaled using the SMART and SAINT software package,²⁴ and the data were corrected for absorption using the SADABS program.²⁵ Pertinent crystallographic data for compounds **1–3**, **5**, and **7** are summarized in Table 4. The structures were solved and refined

(24) SAINT+ Software for CCD Diffractometers; Bruker AXS, Madison, WI, 2000.

(25) Sheldrick, G. M. SADABS Program for Correction of Area Detector Data; University of Göttingen, Göttingen, Germany, 1999.

using the SHELX suite of programs,²⁶ while additional crystallographic calculations were performed by the program PLATON.²⁷ Figures were drawn using ORTEP32.²⁸ The hydrogen atoms were included in geometrically calculated positions in the final stages of the refinement and were refined according to the “riding model”. For compounds **1–3**, all non-hydrogen atoms were refined with anisotropic thermal parameters, with the sole exception of C15 in **2**. The “SQUEEZE” option in PLATON was used to remove a disordered solvent molecule from the overall intensity data of compounds **3** and **7**. The disordered CH_2Cl_2 in **5** was modeled satisfactorily. All non-hydrogen atoms, except the C and Cl atoms of the disordered solvent molecule, were refined anisotropically.

Acknowledgment. We thank the DST India for financial support of this work.

Supporting Information Available: Text and figures giving details on the syntheses and ^1H NMR data for the ligands, CIF files giving X-ray crystallographic data for compounds **1–3**, **5**, and **7**, and a figure showing the contour surface of the σ^* (LUMO) and π^* (HOMO) in $[\text{Ru}_2(3\text{-MeNP})_2(\text{CO})_4]^{2+}$ (3-MeNP = 3-methyl-1,8-naphthyridine). This material is available free of charge via the Internet at <http://pubs.acs.org>.

OM060774+

(26) (a) SHELXTL Package, version 6.10; Bruker AXS, Madison, WI, 2000. (b) Sheldrick, G. M. SHELXS-86 and SHELXL-97; University of Göttingen, Göttingen, Germany, 1997.

(27) Spek, L. PLATON; University of Utrecht, Utrecht, The Netherlands, 2001.

(28) Farrugia, L. J. *J. Appl. Crystallogr.* **1997**, *30*, 565.